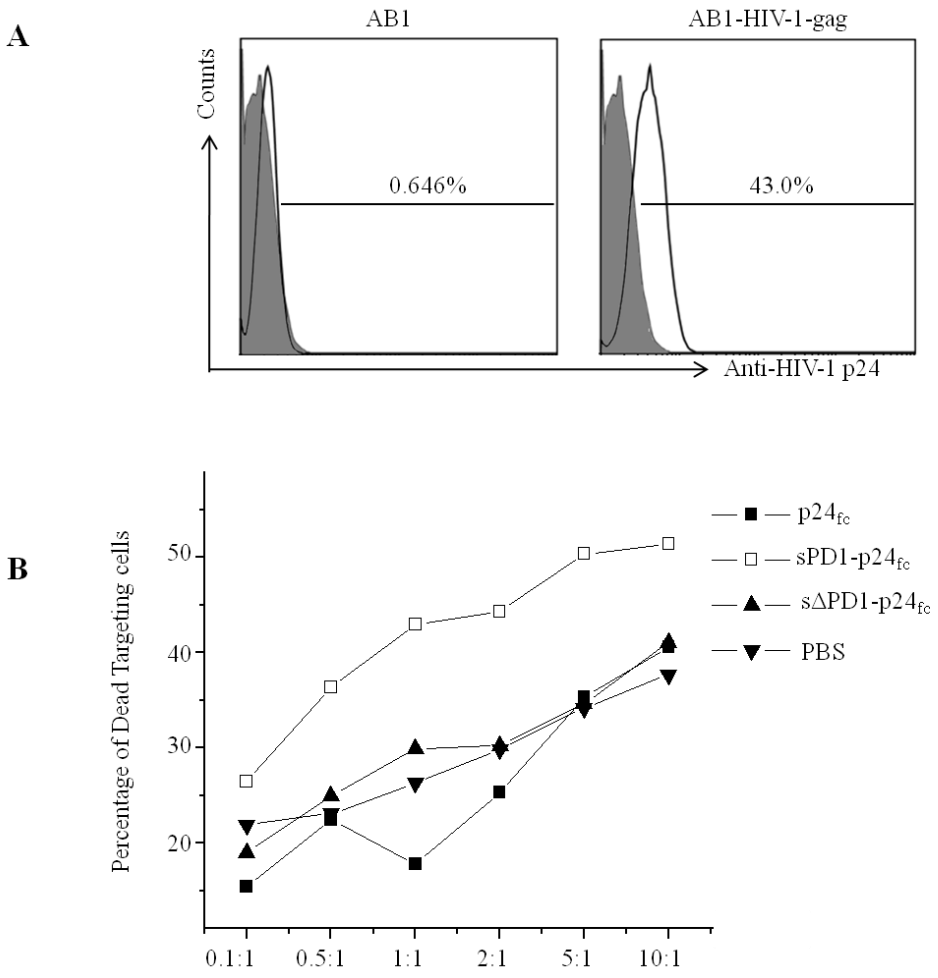

Supplementary Figure 1.

Splenocytes in sPD1-$p24_{fc}$/EP immunized mice shows cytotoxicity efficiency. To determine the cytolytic effects of splenocytes, a mouse mesothelioma cell line AB1 was engineered to stably express HIV-1 Gag. (A) HIV-1 Gag p24 expression on the unmodified AB1 or AB1-HIV-1-Gag cell line were detected by flow cytometry (solid line) with isotype control (shaded). (B) Splenocytes isolated from mice immunized with sPD1-$p24_{fc}$, and sΔPD1-$p24_{fc}$, $p24_{fc}$, or PBS were pre-treated by p24 peptides pool plus anti-CD28 over night before co-cultured with AB1-HIV-1-gag cells at different ratios of effector:target cells. Percentage of dead target cells are presented as a line graph of data representative from three independent experiments.

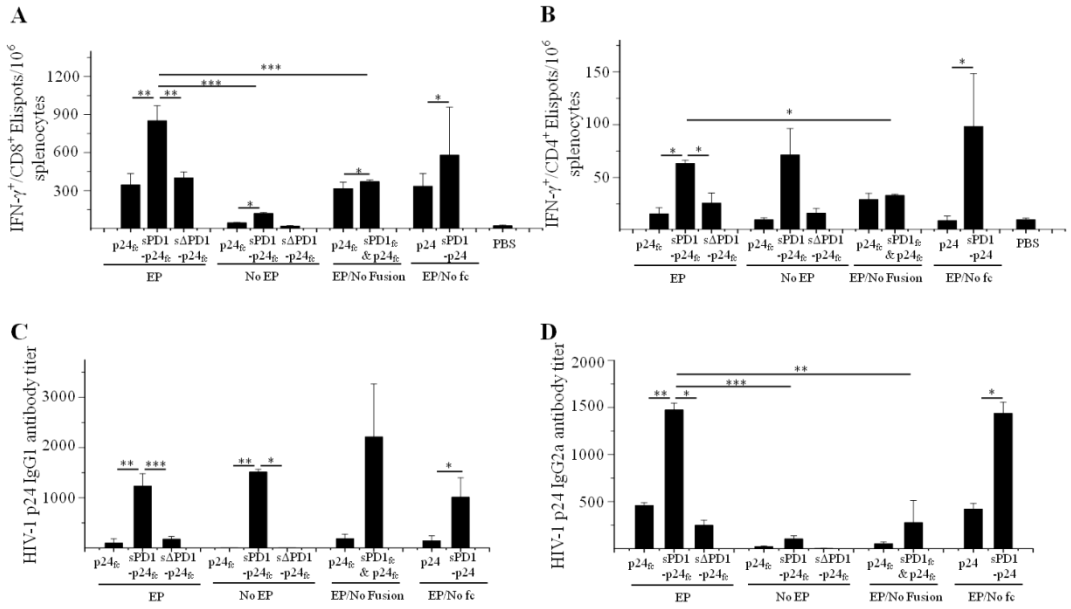

Supplementary Figure 2.

Characterization of sPD1-$p24_{fc}$ DNA vaccination. DNA vaccination by i.m. were performed in different conditions: EP cooperation at 20 μg dose of DNA (EP), without EP at 100 μg (No EP), with 20 μg $p24_{fc}$ and/or 20 μg $sPD1_{fc}$ with EP (EP/No Fusion), or removal of the rabbit Fc tag in all the DNA vaccines using a dose of 20 μg with EP (EP/No fc). Mice sera and splenocytes were collected two weeks after the final immunization for analysis of antibody and T cell responses, respectively. (A) Number of IFN-γ-secreting $CD8^+$ and (B) $CD4^+$ T cells measured by ELISpot in specific response to HIV-1 Gag p24 epitopes gagAI and gag26, respectively. (C) Detection of specific IgG1 and (D) IgG2a antibodies against HIV-1 Gag p24 by ELISA two weeks post immunization. Bars represent the mean values of groups of three mice with standard error depicted by error bars, of three independent immunization experiments. *P<0.05, **P<0.01, ***P<0.001.

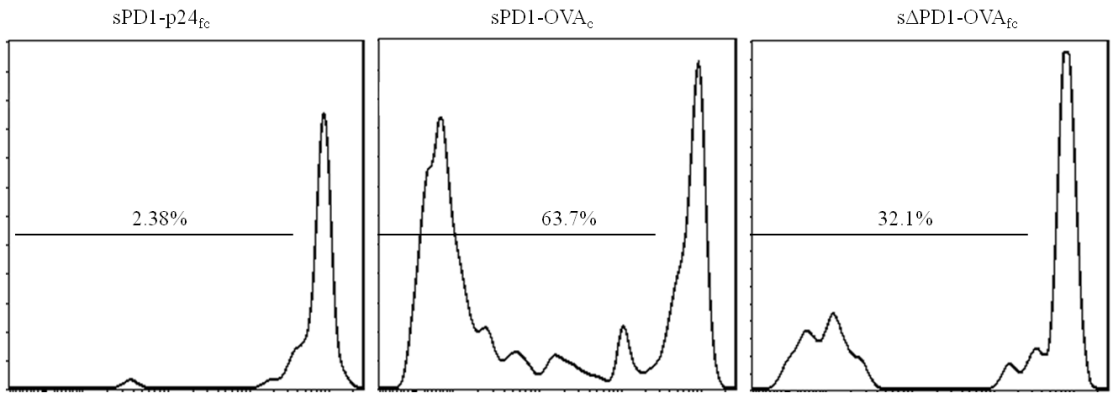

Supplementary Figure 3.

sPD1-based vaccine improves antigen presentation to stimulate $CD8^+$ T cell proliferation in vivo. CFSE-labeled OT-I T cells were adoptively transferred into B6 mice 1 d after i.m./EP injection of sPD1-OVA_{fc} and controls sΔPD1-OVA_{fc} and sPD1-$p24_{fc}$. Five days after immunization, draining lymph nodes were harvested and the extent of proliferation was determined among OT-I cells based on flow cytometric CFSE signals.

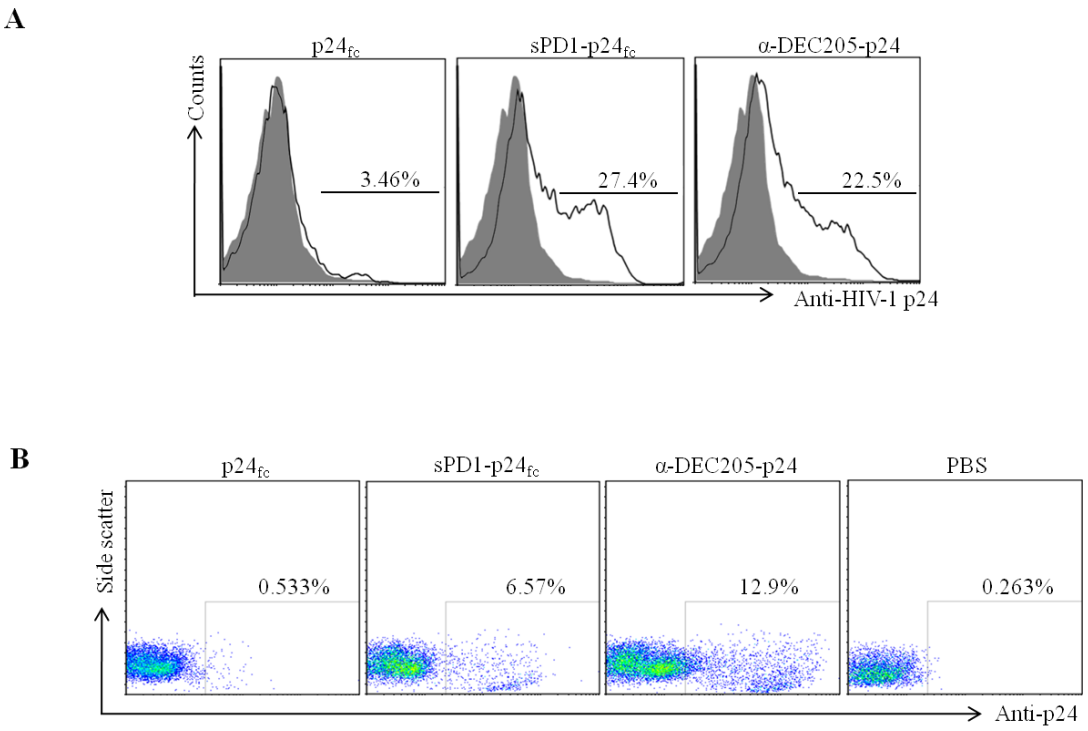

Supplementary Figure 4.

sPD1-p24 is as efficient as anti-DEC205-p24 on binding and antigen uptake ability by $CD11c^+$ DCs. (A) Binding efficiency of purified sPD1-$p24_{fc}$ protein and anti-DEC205-p24 antibody to splenic $CD11c^+$ DCs after 20 min incubation at room temperature. Purified $p24_{fc}$ protein treatment served as negative control. Signals were detected by flow cytometry using anti-HIV-1 p24 antibody (solid line) and DCs without protein treatment was background control (shaded). (B) Intracellular staining of p24 on purified splenic $CD11c^+$ DCs 1h post treated by sPD1-$p24_{fc,}$ anti-DEC205-p24 and $p24_{fc}$. PBS served as negative control. Data generated by flow cytometry to monitor p24 positive signals. Shown data are representative of at least four independent experiments.

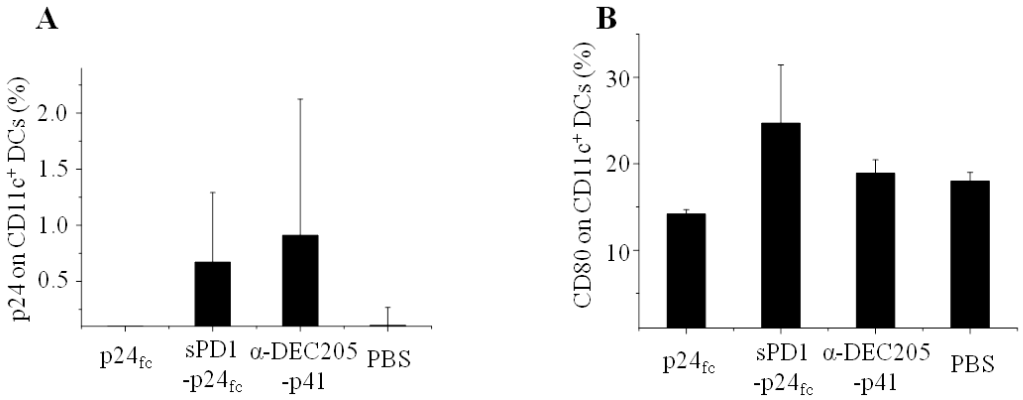

Supplementary Figure 5.

DC-targeting strategy elicited higher maturation stages of DCs than non-targeting $p24_{fc}$ immunization. Mice were immunized with sPD1-$p24_{fc}$, anti-DEC205-p41 and $p24_{fc}$ DNA vaccines, or PBS placebo, at 100 µg i.m./EP. Draining lymph node $CD11c^+$ DCs were examined for (A) Intracellular p24 detection 8h post injection and (B) CD80 24h post injection. Bars represent means of five independently experiments with error bars as standard error.

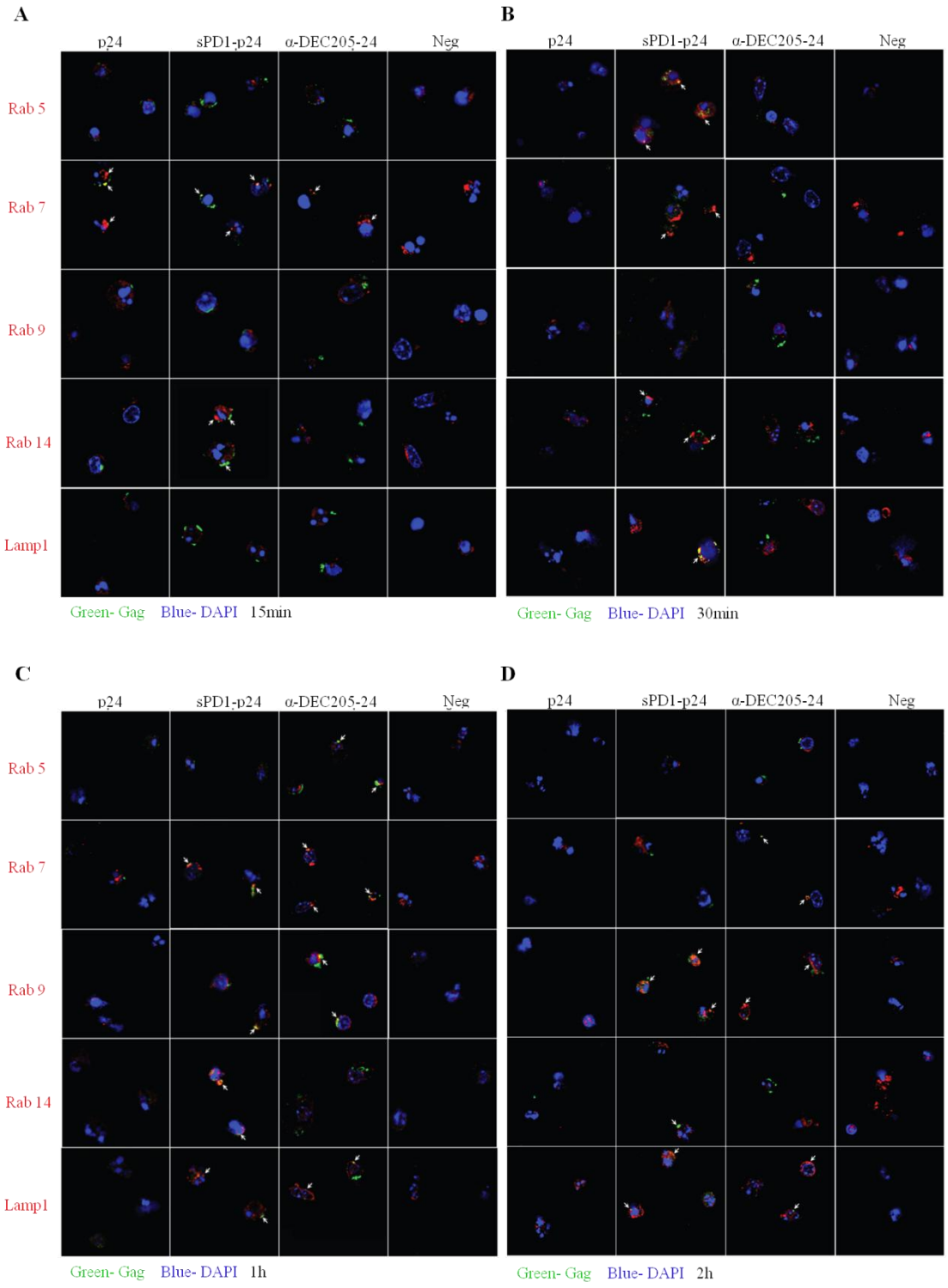

Supplementary Figure 6.

Intracellular routing of antigens in splenic DCs by sPD1-p24 through both early and late endosomes. Purified splenic $CD11c^{+}$ DCs were treated by proteins sPD1-p24,

anti-DEC205-p24 or p24 at 2h and chasing for (A)15min, (B) 30min, (C) 1h and (D) 2h. Formaldehyde-fixed DCs were incubated with primary antibodies against HIV-1 p24, Rab5, Rab7, Rab 9, Rab 14 and Lamp1 antibodies, followed by secondary anti-mouse IgG 488 or anti-rabbit IgG 555. Nuclei were counterstained with DAPI. Images were acquired using Carl Zeiss LSM 700 microscope. Shown are merged images of DCs pulsed with green-stained p24 and red-stained for each endosomal compartment.

15 min

Rab14	p24	sPD1-p24	α-DEC-p24	Neg	Lamp1	p24	sPD1-p24	α-DEC-p24	Neg
Pearson's coefficient	0.007	0.196	0.052	0	Pearson's Co-efficient	0	0.021	0.0345	0.013
Overlap coefficient	0.008	0.102	0.024	0	Overlap co-efficient	0	0.026	0.042	0.013
Mander's coefficient (green/red)	0.361	0.773	0.246	0.182	Mander's coefficient (green/red)	0.01	0.272	0.279	0.426
Mander's coefficient (red/green)	0.001	0.149	0.034	0	Mander's coefficient (red/green)	0.002	0.018	0.032	0.002

30 min

Rab14	p24	sPD1-p24	α-DEC-p24	Neg	Lamp1	p24	sPD1-p24	α-DEC-p24	Neg
Pearson's Co-efficient	0.057	0.226	0.069	0.047	Pearson's Co-efficient	0.158	0.639	0.004	0.02
Overlap co-efficient	0.065	0.249	0.066	0.057	Overlap co-efficient	0.168	0.644	0.012	0.025
Mander's coefficient (green/red)	0.294	0.421	0.707	0.434	Mander's coefficient (green/red)	0.503	0.903	0.122	0.503
Mander's coefficient (red/green)	0.181	0.359	0.017	0.085	Mander's coefficient (red/green)	0.253	0.715	0.011	0.013

1 h

Rab14	p24	sPD1-p24	α-DEC-p24	Neg	Lamp1	p24	sPD1-p24	α-DEC-p24	Neg
Pearson's Co-efficient	0.074	0.507	0.060	0.011	Pearson's Co-efficient	0.123	0.635	0.407	0.037
Overlap co-efficient	0.092	0.523	0.078	0.015	Overlap co-efficient	0.146	0.658	0.104	0.038
Mander's coefficient (green/red)	0.134	0.991	0.389	0.099	Mander's coefficient (green/red)	0.229	0.878	0.938	0.372
Mander's coefficient (red/green)	0.28	0.594	0.054	0.346	Mander's coefficient (red/green)	0.221	0.904	0.127	0.023

2 h

Rab14	p24	sPD1-p24	α-DEC-p24	Neg	Lamp1	p24	sPD1-p24	α-DEC-p24	Neg
Pearson's Co-efficient	0.025	0.161	0.002	0.001	Pearson's Co-efficient	0	0.308	0.130	0.002
Overlap co-efficient	0.027	0.164	0.006	0.001	Overlap co-efficient	0	0.313	0.065	0.002
Mander's coefficient (green/red)	0.148	0.429	0.12	0.018	Mander's coefficient (green/red)	0	0.478	0.921	0.034
Mander's coefficient (red/green)	0.108	0.329	0.007	0.006	Mander's coefficient (red/green)	0	0.684	0.046	0.015

Supplementary Table 1.

Co-localization coefficients. ImageJ (http://imagej.nih.gov/ij/, 1997-2012) with JACoP plug-in was used to calculate various co-localization coefficients – Pearson's correlation, overlap coefficient, and Manders coefficient. The numbers in red denote the most important differences.